

Enhanced violation of Leggett-Garg Inequality in three flavour neutrino oscillations via non-standard interactions

Sheeba Shafaq^{§ a} and Poonam Mehta^{§ b}

[§] *School of Physical Sciences,
Jawaharlal Nehru University, New Delhi 110067, India*

Abstract

Neutrino oscillations occur due to non-zero masses and mixings and most importantly they are believed to maintain quantum coherence even over astrophysical length scales. In the present study, we explore the quantumness of three flavour neutrino oscillations by studying the extent of violation of Leggett-Garg inequalities (LGI) if non-standard interactions are taken into account. We report an enhancement in violation of LGI with respect to the standard scenario for appropriate choice of NSI parameters.

^aEmail: sheebakhawaja7@gmail.com

^bEmail: pm@jnu.ac.in

1 Introduction

Even though quantum mechanics was born in nineteen twenties [1], several significant, conceptual and foundational developments which stem from quantum mechanics emerged much later. The Aharonov-Bohm effect was understood in the sixties [2], Bell's inequalities [3] and the issue of entanglement were appreciated in seventies and developments related to the Leggett-Garg inequalities (LGI) [4] emerged in the eighties. In their seminal paper, Leggett and Garg [4] derived a class of inequalities which provided a way to test the applicability of quantum mechanics as we go from the microscopic to the macroscopic world. The work was based on our intuition about the macroscopic world which can be defined in terms of the two principles : (a) Macroscopic realism (MR) which implies that the performance of a measurement on a macroscopic system reveals a well-defined pre-existing value (b) Non-invasive measurability (NIM) which states that in principle, we can measure this value without disturbing the system. The classical world, in general, respects both these assumptions. However, in quantum mechanics, both the assumptions are violated as it is based on superposition principle and collapse of wave function under measurement (see [5] for a review). There exists a maximum quantum-mechanical value of the LGI correlator with the standard measurement protocol and this is referred to as Luder's bound or temporal Tsirelson's bounds [6–9]. LGIs can be used as indicators of quantum coherence, specifically for macroscopic systems. Apart from LGI, there are other useful measures which prove useful to quantify quantumness such as quantum witness, contextuality etc [10–14].

If we look at the developments in the neutrino sector, soon after the discovery of the second type of neutrino in the sixties, the idea of neutrino flavour oscillations was proposed [15–18]. The experimental vindication of the idea of neutrino flavour oscillations took several decades and was rewarded with the 2015 Nobel Prize for Physics [19]. Neutrino oscillations among the three active flavours imply that at least two of the neutrino states are massive which can not be reconciled within the Standard Model of particle physics. The phenomenon of neutrino flavour oscillation arises from the phase difference acquired by the mass eigenstates due to their time evolution during propagation in vacuum or matter [20]. The idea of non-standard interactions (NSI) originated in the seminal work of Wolfenstein as a viable alternative to mass-induced oscillations [21] (see also [22–25]). Of course, now we know that standard mass-induced neutrino oscillations have been firmly established yet sub-dominant effects due to NSI can impact measurements at current and future oscillation experiments. There are strong reasons to believe that sub-dominant effects due to neutrino NSI could cause interference with the standard oscillation measurements and neutrino NSI is the most studied new physics topic in the current times (see [26–28] for reviews). Recent studies have demonstrated that the discrepancy arising in data from two of the long baseline neutrino experiments, T2K and NoVA can be reconciled by invoking large NSI [29, 30].

Given that neutrinos exhibit sustained quantum coherence even over astrophysical length scales, it is natural to explore geometric aspects of the phases involved [31] as well as think about quantification of the coherence properties of neutrinos via temporal correlations in the form of LGI. Study of temporal correlations in the form of LGI has attracted significant attention in recent times both in the context of two [32–34] and three [35–38] flavour neutrino oscillations. It should be noted that while different dichotomic observables have been employed in these studies, the neutrino matter interactions have been considered to be

standard in these studies.

Before we proceed to describe the key idea of the present work, we would like to summarize the existing work on LGI in the context of neutrino oscillations. In one of the early attempts [32], the authors considered LGI in the context of two state oscillations of neutral kaons and neutrinos. The implication of neutrino oscillations on LGI was characterized by a quantity K_4 which was found to be sensitive to the mixing angle appearing in two flavour neutrino oscillations and the conclusion was that it could reach its upper bound of $2\sqrt{2}$ for a specific value of the mixing angle, $\theta = \pi/4$. Observation of violation of LGI was reported for the first time in the context of Main Injector Neutrino Oscillation Search (MINOS) experiment [33]. The large ($\sim 6\sigma$) violation in this microscopic system of neutrinos over a macroscopic distance of 735 km provided the longest range over which a temporal analogue of Bell's test of quantum mechanics had been performed. Soon after, observation of $\sim 6\sigma$ violation of LGI in the experimental data obtained at Daya Bay reactor experiment was reported [34]. It should be remarked that all the above studies were performed assuming two neutrino states only and therefore obscured the parameter dependencies present in the three flavour analysis. In order to shed some light on the dependence on CP phase and other parameter dependencies via LGI, it becomes imperative to perform the analysis taking three flavour neutrino oscillations into account. The three flavour analysis was first carried out in [35] in which condition for attaining maximum violation of LGI was laid down. Moreover, it was concluded that non-zero three flavour oscillation parameters such as θ_{13} , the CP phase (δ), the mass ordering parameter (α) led to an enhanced violation of LGI in comparison to the two flavour case. Additionally, three flavour analysis has been carried out assuming stationarity condition [36] and relaxing it [37]. With the stationarity assumption, it was shown that the quantity representing LGI has a sensitive dependence on the neutrino mass ordering [36]. Various inequivalent forms of LGI in subatomic systems have been explored in [38].

Using the tools of quantum resource theory [10, 11], the authors of Ref. [39, 40] quantified the quantumness of experimentally observed neutrino oscillations. The authors in [39] analysed ensembles of reactor and accelerator neutrinos at distinct energies from a variety of neutrino sources, including Daya Bay (0.5 km and 1.6 km), Kamland (180 km), MINOS (735 km), and T2K (295 km). Though far-fetched, there was also an idea where it was shown that one could obtain difference in possible violation of LGI depending on the type of neutrinos (Dirac or Majorana) by selecting appropriate quantity for K_3 [41]. Among other measures of coherence in the context of neutrino oscillations, contextuality has been studied in [42] and the l_1 norm of coherence introduced in [10] have been explored in [43, 44]. The entropic uncertainty relations have been investigated by comparing the experimental observation of neutrino oscillations to predictions in [45]. Also, tri-partite entanglement in neutrino oscillations has been studied in [46].

The work of Leggett and Garg [4] is, undoubtedly, one of the most profound developments in the area of foundations of quantum mechanics. The present article weaves together the idea of LGI and neutrino oscillation physics in presence of NSI to explore the extent and possibility of enhancement of violation of LGI in case of three flavour oscillations. Such a type of enhancement is of interest to a wide range of physicists in several areas of physics and in particular, in the area of quantum information and computation. To the best of our knowledge, NSI induced effects on violation of LGI in neutrino sector have not been reported

so far.

The plan of this article is as follows. In Sec. 2, we describe the basic framework which comprises of brief review of the three flavour neutrino oscillations in presence of NSI as well as definition of observables used to quantify the extent of violation of LGI in the context of neutrino oscillations. We describe our results in Sec. 3. Finally, the conclusion and outlook is presented in Sec. 4.

2 Framework

The parameters entering the standard three flavour oscillation framework are : three angles (θ_{12} , θ_{23} , θ_{13}), one phase (δ) as well as the two mass-squared differences ($\Delta m_{21}^2 = m_2^2 - m_1^2$ and $\Delta m_{31}^2 = m_3^2 - m_1^2$). Table 1 summarizes the current values of the parameters (taken from [47]).

Parameter	Best-fit value	3σ interval
θ_{12} [$^\circ$]	34.3	31.4 - 37.4
θ_{13} [$^\circ$] (NO)	8.58	8.16 - 8.94
θ_{13} [$^\circ$] (IO)	8.63	8.21 - 8.99
θ_{23} [$^\circ$] (NO)	48.8	41.63 - 51.32
θ_{23} [$^\circ$] (IO)	48.8	41.88 - 51.30
Δm_{21}^2 [10^{-5}eV^2]	7.5	[6.94 - 8.14]
Δm_{31}^2 [10^{-3}eV^2] (NO)	+2.56	[2.46 - 2.65]
Δm_{31}^2 [10^{-3}eV^2] (IO)	-2.46	-[2.37 - 2.55]
δ [Rad.] (NO)	-0.8π	$[-\pi, 0] \cup [0.8\pi, \pi]$
δ [Rad.] (IO)	-0.46π	$[-0.86\pi, -0.1\pi]$

Table 1: The best-fit and allowed range of the standard oscillation parameters used in our analysis [47].

2.1 Non-standard interactions

Non-standard interactions [21, 23–25] (see [26–28] for reviews) refer to a wide class of new physics scenarios parameterised in a model-independent way at low energies ($E \ll M_{EW}$, where M_{EW} is the electroweak scale) by using effective four-fermion interactions. In general, these NSI can impact the neutrino oscillation signals via charged current (CC) or neutral current (NC) processes. CC interactions affect processes only at the source or the detector which are discernible at near detectors while the NC interactions affect the propagation of neutrinos which can be probed at far detectors. In this work, we consider the NC terms which affect propagation of neutrinos. The effective Lagrangian describing the neutrino NSI

is given by

$$\mathcal{L}_{\text{CC}} = -2\sqrt{2}G_F\varepsilon_{\alpha\beta}^{ff'C}[\bar{\nu}_\alpha\gamma^\mu P_L l_\beta][\bar{f}'\gamma_\mu P_C f], \quad (1)$$

$$\mathcal{L}_{\text{NC}} = -2\sqrt{2}G_F\varepsilon_{\alpha\beta}^{fC}[\bar{\nu}_\alpha\gamma^\mu P_L \nu_\beta][\bar{f}\gamma_\mu P_C f]. \quad (2)$$

where G_F is the Fermi constant, α, β denote lepton flavours and f is the first¹ generation fermion (e, u, d). The dimensionless coefficients, $\varepsilon_{\alpha\beta}^{ff'C}$ or $\varepsilon_{\alpha\beta}^{fC}$ quantify the strength of the NSI with respect to the standard weak interaction. Here f and f' denote the charged fermions involved in the interactions with background fermions. The chirality projection operators are given by $P_L = (1-\gamma_5)/2$ and $P_C = (1\pm\gamma_5)/2$. It should be noted that only the incoherent sum of all individual contributions (e, u, d) impacts the coherent forward scattering of neutrinos on matter. Normalizing to n_e , the effective NSI parameter for neutral Earth matter is

$$\varepsilon_{\alpha\beta} = \sum_{f=e,u,d} \frac{n_f}{n_e} \varepsilon_{\alpha\beta}^f = \varepsilon_{\alpha\beta}^e + 2\varepsilon_{\alpha\beta}^u + \varepsilon_{\alpha\beta}^d + \frac{n_n}{n_e} (2\varepsilon_{\alpha\beta}^d + \varepsilon_{\alpha\beta}^u) = \varepsilon_{\alpha\beta}^e + 3\varepsilon_{\alpha\beta}^u + 3\varepsilon_{\alpha\beta}^d, \quad (3)$$

where n_f is the density of fermion f in medium traversed by the neutrino and n refers to neutrons. Also, NC type NSI matter effects are sensitive only to the vector sum of NSI couplings, *i.e.*, $\varepsilon_{\alpha\beta}^f = \varepsilon_{\alpha\beta}^{fL} + \varepsilon_{\alpha\beta}^{fR}$.

As far as CC NSI terms are concerned, those are tightly constrained [48]. The constraints on NC type NSI parameters are less stringent. As mentioned above, the combination that enters oscillation physics is given by Eq. (3). The individual NSI terms such as $\varepsilon_{\alpha\beta}^{fL}$ or $\varepsilon_{\alpha\beta}^{fR}$ are constrained in any experiment (keeping only one of them non-zero at a time) and moreover the coupling is either to e, u, d individually [48]. In view of this, it is not so straightforward to interpret those bounds in terms of an effective $\varepsilon_{\alpha\beta}$. One could take the conservative approach *i.e.*, use the most stringent constraint on individual NSI terms. Using this, it is found that the NSI parameters involving the muon sector are more tightly constrained than the electron or tau sector ($|\varepsilon_{\mu\mu}| < 0.003$, $|\varepsilon_{\mu\tau}| < 0.05$, $|\varepsilon_{e\mu}| < 0.05$, $|\varepsilon_{e\tau}| < 0.27$, $|\varepsilon_{ee}| < 0.06$, $|\varepsilon_{\tau\tau}| < 0.16$) [48]. However, the authors in Ref. [49] deduced model-independent bounds (assuming that the errors on individual NSI terms are not correlated) on effective NC NSI terms given by $\varepsilon_{\alpha\beta} \lesssim \left\{ \sum_{C=L,R} [(\varepsilon_{\alpha\beta}^{eC})^2 + (3\varepsilon_{\alpha\beta}^{uC})^2 + (3\varepsilon_{\alpha\beta}^{dC})^2] \right\}^{1/2}$. For neutral Earth matter, we have

$$|\varepsilon_{\alpha\beta}| < \begin{pmatrix} 4.2 & 0.33 & 3.0 \\ 0.33 & 0.068 & 0.33 \\ 3.0 & 0.33 & 21 \end{pmatrix}.$$

The values of NSI parameters considered in this work are well within these constraints.

In the ultra-relativistic limit, the neutrino propagation is governed by a Schrödinger-type equation with an effective Hamiltonian

$$\mathcal{H} = \mathcal{H}_{\text{vac}} + \mathcal{H}_{\text{SI}} + \mathcal{H}_{\text{NSI}}, \quad (4)$$

where \mathcal{H}_{vac} , \mathcal{H}_{SI} and \mathcal{H}_{NSI} represent the Hamiltonian in vacuum and in presence of SI and NSI, respectively. Thus,

¹Matter contains only first generation fermions and hence second or third generation fermions do not affect oscillation experiments.

$$\mathcal{H} = \frac{1}{2E} \left\{ \mathcal{U} \begin{pmatrix} 0 & & \\ & \Delta m_{21}^2 & \\ & & \Delta m_{31}^2 \end{pmatrix} \mathcal{U}^\dagger + A(x) \begin{pmatrix} 1 & & \\ & 0 & \\ & & 0 \end{pmatrix} + A(x) \begin{pmatrix} \varepsilon_{ee} & \varepsilon_{e\mu} & \varepsilon_{e\tau} \\ \varepsilon_{e\mu}^* & \varepsilon_{\mu\mu} & \varepsilon_{\mu\tau} \\ \varepsilon_{e\tau}^* & \varepsilon_{\mu\tau}^* & \varepsilon_{\tau\tau} \end{pmatrix} \right\}, \quad (5)$$

where $A(x) = 2E\sqrt{2}G_F n_e(x)$ is the standard CC potential due to the coherent forward scattering of neutrinos. The three flavour neutrino mixing matrix $\mathcal{U} \equiv \mathcal{U}_{23}\mathcal{W}_{13}\mathcal{U}_{12}$ with $\mathcal{W}_{13} = \mathcal{U}_\delta \mathcal{U}_{13} \mathcal{U}_\delta^\dagger$ and $\mathcal{U}_\delta = \text{diag}\{1, 1, \exp(i\delta)\}$ is characterized by three angles and a single (Dirac) phase and, in the standard Pontecorvo-Maki-Nakagawa-Sakata (PMNS) parameterisation, we have

$$\mathcal{U} = \begin{pmatrix} 1 & 0 & 0 \\ 0 & c_{23} & s_{23} \\ 0 & -s_{23} & c_{23} \end{pmatrix} \begin{pmatrix} c_{13} & 0 & s_{13}e^{-i\delta} \\ 0 & 1 & 0 \\ -s_{13}e^{i\delta} & 0 & c_{13} \end{pmatrix} \begin{pmatrix} c_{12} & s_{12} & 0 \\ -s_{12} & c_{12} & 0 \\ 0 & 0 & 1 \end{pmatrix}, \quad (6)$$

where $s_{ij} = \sin\theta_{ij}$, $c_{ij} = \cos\theta_{ij}$. It should be noted that two Majorana phases do not play any role in neutrino oscillations, and hence not considered.

In order to elucidate the role of different NSI terms in a particular oscillation channel, we can obtain approximate analytic expressions for oscillation probabilities corresponding to various channels using techniques of perturbation theory. The analytic computation of probability expressions in presence of NSI has been carried out for different experimental settings [50–52]. Let us define the following ratios for the sake of convenience,

$$\lambda \equiv \frac{\Delta m_{31}^2}{2E} \quad ; \quad r_\lambda \equiv \frac{\Delta m_{21}^2}{\Delta m_{31}^2} \quad ; \quad r_A \equiv \frac{A(x)}{\Delta m_{31}^2}. \quad (7)$$

The expressions given below are valid for atmospheric and long baseline neutrinos where $\lambda L \simeq \mathcal{O}(1)$ holds and $r_A L \sim \mathcal{O}(1)$ for a large range of the E and L values. The $\nu_\mu \rightarrow \nu_e$ oscillation probability is given by

$$\begin{aligned} P_{\mu e}^{NSI} \simeq & 4s_{13}^2 s_{23}^2 \left[\frac{\sin^2(1 - r_A)\lambda L/2}{(1 - r_A)^2} \right] \\ & + 8s_{13}s_{23}c_{23}(|\varepsilon_{e\mu}|c_{23}c_\chi - |\varepsilon_{e\tau}|s_{23}c_\omega)r_A \left[\frac{\sin r_A \lambda L/2}{r_A} \frac{\sin(1 - r_A)\lambda L/2}{(1 - r_A)} \cos \frac{\lambda L}{2} \right] \\ & + 8s_{13}s_{23}c_{23}(|\varepsilon_{e\mu}|c_{23}s_\chi - |\varepsilon_{e\tau}|s_{23}s_\omega)r_A \left[\frac{\sin r_A \lambda L/2}{r_A} \frac{\sin(1 - r_A)\lambda L/2}{(1 - r_A)} \sin \frac{\lambda L}{2} \right] \\ & + 8s_{13}s_{23}^2(|\varepsilon_{e\mu}|s_{23}c_\chi + |\varepsilon_{e\tau}|c_{23}c_\omega)r_A \left[\frac{\sin^2(1 - r_A)\lambda L/2}{(1 - r_A)^2} \right], \end{aligned} \quad (8)$$

where we have used $\tilde{s}_{13} \equiv \sin\tilde{\theta}_{13} = s_{13}/(1 - r_A)$ to the leading order in s_{13} , and $\chi = \phi_{e\mu} + \delta$, $\omega = \phi_{e\tau} + \delta$. Only the parameters $\varepsilon_{e\mu}$ and $\varepsilon_{e\tau}$ enter in the leading order expression [50–52], as terms such as $r_\lambda \varepsilon_{\alpha\beta}$ have been neglected.

The muon neutrino survival probability ($\nu_\mu \rightarrow \nu_\mu$) is given by

$$\begin{aligned}
P_{\mu\mu}^{NSI} \simeq & 1 - s_{2\times 23}^2 \left[\sin^2 \frac{\lambda L}{2} \right] \\
& - |\varepsilon_{\mu\tau}| \cos \phi_{\mu\tau} s_{2\times 23} \left[s_{2\times 23}^2 (r_A \lambda L) \sin \lambda L + 4c_{2\times 23}^2 r_A \sin^2 \frac{\lambda L}{2} \right] \\
& + (|\varepsilon_{\mu\mu}| - |\varepsilon_{\tau\tau}|) s_{2\times 23}^2 c_{2\times 23} \left[\frac{r_A \lambda L}{2} \sin \lambda L - 2r_A \sin^2 \frac{\lambda L}{2} \right], \quad (9)
\end{aligned}$$

where $s_{2\times 23} \equiv \sin 2\theta_{23}$ and $c_{2\times 23} \equiv \cos 2\theta_{23}$. Note that the NSI parameters involving the electron sector do not enter this channel and the survival probability depends only on the three parameters $\varepsilon_{\mu\mu}, \varepsilon_{\mu\tau}, \varepsilon_{\tau\tau}$.

2.2 Leggett-Garg Inequalities

In order to write down an expression for LGI, we require correlation functions $C_{ij} = \langle \hat{Q}(t_i) \hat{Q}(t_j) \rangle$ of a dichotomic observable, $\hat{Q}(t)$ (with realizations ± 1) at distinct measurement times t_i and t_j . Here, $\langle \dots \rangle$ implies averaging over many trials. As stated in [4], the actual derivation of LGIs relied on the assumption that measurements of \hat{Q} at different times t_i are carried out in non-invasive manner. However, one may relax this and assume stationarity in which case C_{ij} depend only on the time difference $\tau = t_j - t_i$ [5]. In terms of the joint probabilities, the two-time correlation function can be expressed as

$$C_{ij} = \sum_{\hat{Q}_i \hat{Q}_j = \pm 1} \hat{Q}_i \hat{Q}_j \mathbb{P}_{\hat{Q}_i \hat{Q}_j}(t_i, t_j) \quad (10)$$

where $\mathbb{P}_{\hat{Q}_i \hat{Q}_j}(t_i, t_j)$ is the joint probability of obtaining the results \hat{Q}_i and \hat{Q}_j from successive measurements at times t_i and t_j , respectively. For n -time measurement, we can define the parameter K_n as

$$K_n \equiv \sum_{i=1}^{n-1} C_{i,i+1} - C_{1,n} \quad (11)$$

Note that K_n quantifies the extent of violation of LGI.

The simplest LGIs are for three-time and four-time measurements (K_3 and K_4), which can be expressed as [5]

$$\begin{aligned}
-3 \leq K_3 \leq 1 \quad \text{where} \quad K_3 &= C_{12} + C_{23} - C_{13} \\
-2 \leq K_4 \leq 2 \quad \text{where} \quad K_4 &= C_{12} + C_{23} + C_{34} - C_{14}
\end{aligned} \quad (12)$$

The generalization for the case of n -time measurements leads to

$$\begin{aligned}
-n \leq K_n \leq n-2 \quad & \text{for odd values of } n (\geq 3) \\
-(n-2) \leq K_n \leq n-2 \quad & \text{for even values of } n (\geq 4)
\end{aligned} \quad (13)$$

Thus, for n -time measurements with $n \geq 3$, $K_n \leq n-2$ for any value of n . These inequalities have been tested in many experiments and are found to be violated [5]. The maximum quantum-mechanical value of the LGI correlator with the standard measurement protocol is

$$K_3^{max} = \frac{3}{2} \quad \text{and} \quad K_4^{max} = 2\sqrt{2} \quad (14)$$

These bounds (referred to as Luder's bound or temporal Tsirelson's bounds [6–9]) are analogous to Tsirelson bounds in the context of spatially separated observations.

Let us try to explain the sense of these bounds for the lowest order LGI parameter, K_3 . First of all, $-3 \leq K_3 \leq 3$ is the algebraic bound since C_{ij} can take values ± 1 . The bounds in Eq. 12, *i.e.*, $-3 \leq K_3 \leq 1$ imply that (a) the underlying dynamics classical (*i.e.*, macroscopic realism and NIM hold), or (b) even if the dynamics is quantum, it does not violate macroscopic realism and NIM which are expected to hold for classical dynamics. So, in this sense, this represents the classical bound. If the two conditions (*i.e.*, macroscopic realism and NIM) are violated then the dynamics is quantum and we expect $1 < K_3 \leq 1.5$ and the upper bound in this case is called the Luder's bound or temporal Tsirelson's bound as stated above. Hence, the LGI parameter values lying outside the classical limits (*i.e.*, if $1 \leq K_3 \leq 1.5$) are indicative of the quantumness.

2.3 Neutrino oscillations and LGI violation

In sharp contrast to the electronic or photonic systems, neutrinos exhibit coherence over astrophysical length scales which offers us a unique setting to test LGI in neutrino oscillations. Tests of LGI have been carried out on neutrinos [33, 34]. Let us describe the formalism to compute the joint probabilities for two- and three- flavour neutrino oscillations.

The initial state is taken to be $|\nu_e\rangle$. Electron neutrinos could be produced in the Beta beam set-up [53]. The dichotomic observable, \hat{Q} assumes value $+1$ if neutrino is electron flavoured, $|\nu_e\rangle$. \hat{Q} assumes value -1 if neutrino is muon flavoured, $|\nu_\mu\rangle$ (or tau flavoured, $|\nu_\tau\rangle$ in the three flavour case).

We first briefly review the simplest case of two flavour neutrino oscillations in vacuum. We can express C_{12} as

$$C_{12} = \mathbb{P}_{\nu_e\nu_e}(t_1, t_2) - \mathbb{P}_{\nu_e\nu_\mu}(t_1, t_2) - \mathbb{P}_{\nu_\mu\nu_e}(t_1, t_2) + \mathbb{P}_{\nu_\mu\nu_\mu}(t_1, t_2)$$

where $\mathbb{P}_{\nu_\alpha\nu_\beta}(t_1, t_2) = P_{\nu_e \rightarrow \nu_\alpha}(t_1)P_{\nu_\alpha \rightarrow \nu_\beta}(t_2)$ is the joint probability of obtaining neutrino in state $|\nu_\alpha\rangle$ at time t_1 and in state $|\nu_\beta\rangle$ at time t_2 . Using the two flavour probability expressions in vacuum [20], it can be shown that C_{12} takes the form [32]

$$C_{12} = 1 - 2 \sin^2 2\theta \sin^2 \left(\frac{\lambda}{2} \Delta L \right) \quad (15)$$

where $\Delta L \equiv L_2 - L_1$ (with L_1 and L_2 being the distance from the source at which measurements take place) has been used in place of $\tau \equiv t_2 - t_1$ (in the ultra-relativistic limit, we use the substitution $t \rightarrow L$). Thus, we note that in the two flavour case, C_{12} depends only on $\Delta L \equiv L_2 - L_1$ and not on individual L_1 or L_2 , thereby respecting the stationarity condition

naturally. We can compute the other C_{ij} 's in a similar way and evaluate K_4 . If we take all separations to be equal, i.e., $L_2 - L_1 = L_3 - L_2 = L_4 - L_3 \equiv \Delta L$, we have $C_{12} = C_{23} = C_{34}$. Under this assumption, K_4 is given by

$$K_4 = 2 - 2 \sin^2 2\theta \left[3 \sin^2 \left(\frac{\lambda}{2} \Delta L \right) - \sin^2 \left(\frac{3\lambda}{2} \Delta L \right) \right] \quad (16)$$

Interestingly, it can be noted from Eq. 16, that K_4 is an oscillatory function of $\Delta L/E$. We will demonstrate this in Sec. 3.

The earth matter effects (both SI and NSI) modify the effective angle, $\theta \rightarrow \tilde{\theta}$ and mass-squared difference, $\Delta m^2 \rightarrow \tilde{\Delta m^2}$, but the form of probabilities remain [20] and therefore C_{12} (and K_4) in matter will also have the same form as in vacuum (see Eqs. 15 and 16) and consequently, stationarity will remain preserved even in presence of matter.

In the context of three flavour neutrino oscillations in matter, C_{12} can be written down in terms of the nine joint probabilities [35],

$$C_{12} = \mathbb{P}_{\nu_e \nu_e}(L_1, L_2) - \mathbb{P}_{\nu_e \nu_\mu}(L_1, L_2) - \mathbb{P}_{\nu_e \nu_\tau}(L_1, L_2) - \mathbb{P}_{\nu_\mu \nu_e}(L_1, L_2) + \mathbb{P}_{\nu_\mu \nu_\mu}(L_1, L_2) \\ + \mathbb{P}_{\nu_\mu \nu_\tau}(L_1, L_2) - \mathbb{P}_{\nu_\tau \nu_e}(L_1, L_2) + \mathbb{P}_{\nu_\tau \nu_\mu}(L_1, L_2) + \mathbb{P}_{\nu_\tau \nu_\tau}(L_1, L_2) \quad (17)$$

where $\mathbb{P}_{\nu_\alpha \nu_\beta}(L_1, L_2) = P_{\nu_e \rightarrow \nu_\alpha}(L_1) P_{\nu_\alpha \rightarrow \nu_\beta}(L_2)$ is the joint probability of obtaining a neutrino in state $|\nu_\alpha\rangle$ at L_1 and in state $|\nu_\beta\rangle$ at L_2 . Using the approximate expressions of oscillation probabilities in matter with SI, it is straightforward but somewhat tedious to compute C_{12} and other correlation functions. C_{12} is given by

$$C_{12} = \left[1 - r_\lambda^2 \sin^2 2\theta_{12} \frac{\sin^2 \left(\frac{r_A \lambda L_1}{2} \right)}{(r_A)^2} - 4s_{13}^2 \frac{\sin^2(r_A - 1) \frac{\lambda L_1}{2}}{(r_A - 1)^2} \right] \left[1 - 2r_\lambda^2 \sin^2 2\theta_{12} \frac{\sin^2 \left(\frac{r_A \lambda \Delta L}{2} \right)}{r_A^2} \right. \\ \left. - 8s_{13}^2 \frac{\sin^2(r_A - 1) \frac{\lambda \Delta L}{2}}{(r_A - 1)^2} \right] - \left[r_\lambda^2 \sin^2 2\theta_{12} c_{23}^2 \frac{\sin^2 \left(\frac{V L_1}{2} \right)}{r_A^2} + 4s_{13}^2 s_{23}^2 \frac{\sin^2(r_A - 1) \frac{\lambda L_1}{2}}{(r_A - 1)^2} + 2r_\lambda s_{13} \right. \\ \left. \sin 2\theta_{12} \sin 2\theta_{23} \cos \left(\frac{\lambda L_1}{2} - \delta \right) \frac{\sin \left(\frac{r_A \lambda L_1}{2} \right)}{r_A} \frac{\sin(r_A - 1) \frac{\lambda L_1}{2}}{(r_A - 1)} \right] \left[2r_\lambda^2 \sin^2 2\theta_{12} c_{23}^2 \frac{\sin^2 \left(\frac{r_A \lambda \Delta L}{2} \right)}{r_A^2} \right. \\ \left. + 8s_{13}^2 s_{23}^2 \frac{\sin^2(r_A - 1) \frac{\lambda \Delta L}{2}}{(r_A - 1)^2} + 4r_\lambda s_{13} \sin 2\theta_{12} \sin 2\theta_{23} \frac{\sin \left(\frac{r_A \lambda \Delta L}{2} \right)}{r_A} \frac{\sin(r_A - 1) \frac{\lambda \Delta L}{2}}{(r_A - 1)} \right. \\ \left. \times \left\{ \cos \left(\frac{\lambda \Delta L}{2} - \delta \right) - \sin \delta \sin \left(\frac{\lambda \Delta L}{2} \right) \right\} - 1 \right] - \left[r_\lambda^2 \sin^2 2\theta_{12} s_{23}^2 \frac{\sin^2 \left(\frac{r_A \lambda L_1}{2} \right)}{r_A^2} + 4s_{13}^2 c_{23}^2 \right. \\ \left. \times \frac{\sin^2(r_A - 1) \frac{\lambda L_1}{2}}{(r_A - 1)^2} - 2r_\lambda s_{13} \sin 2\theta_{12} \sin 2\theta_{23} \cos \left(\frac{\lambda L_1}{2} - \delta \right) \frac{\sin \left(\frac{r_A \lambda L_1}{2} \right)}{r_A} \frac{\sin \left\{ (r_A - 1) \frac{\lambda L_1}{2} \right\}}{(r_A - 1)} \right] \\ \left[2r_\lambda^2 \sin^2 2\theta_{12} s_{23}^2 \frac{\sin^2 \left(\frac{r_A \lambda \Delta L}{2} \right)}{r_A^2} + 8s_{13}^2 c_{23}^2 \frac{\sin^2 \left\{ (r_A - 1) \frac{\lambda \Delta L}{2} \right\}}{(r_A - 1)^2} - 4r_\lambda s_{13} \sin 2\theta_{12} \sin 2\theta_{23} \right. \\ \left. \frac{\sin \left(\frac{r_A \lambda \Delta L}{2} \right)}{r_A} \frac{\sin(r_A - 1) \frac{\lambda \Delta L}{2}}{(r_A - 1)} \left\{ \cos \left(\frac{\lambda \Delta L}{2} - \delta \right) - \sin \delta \sin \left(\frac{\lambda \Delta L}{2} \right) \right\} - 1 \right] \quad (18)$$

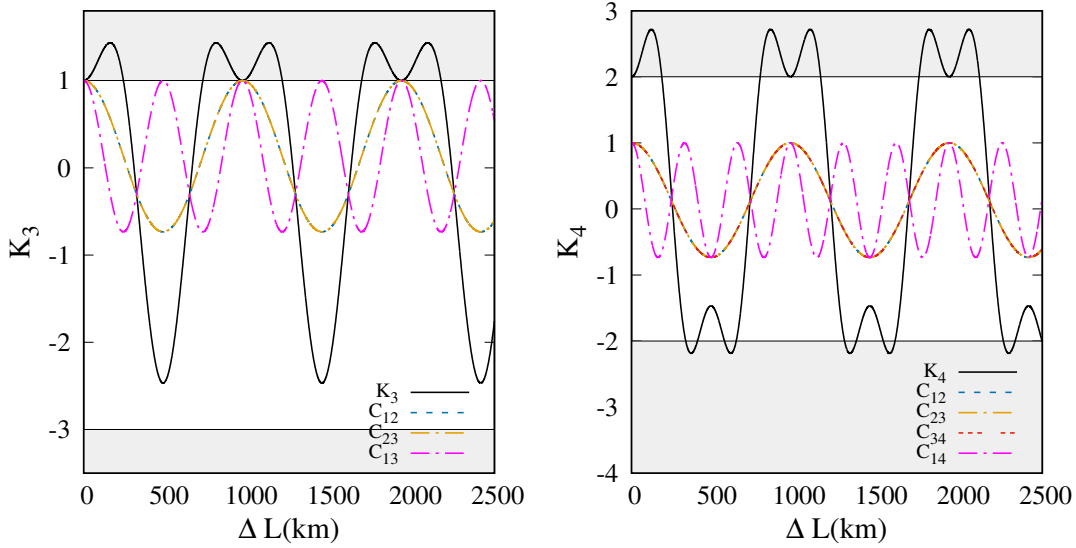


Figure 1: K_3 and K_4 plotted as a function of ΔL for the two flavour neutrino oscillations in vacuum. The contribution of various C_{ij} 's is depicted in the two panels. The grey shaded regions imply violation of LGI in this and the following figures.

We note that C_{12} has explicit dependence on individual baseline, L_1 as well as the spatial separation, $\Delta L = L_2 - L_1$. Thus, stationarity condition is violated in the three flavour case when standard matter interactions are taken into consideration. We can compute the other C_{ij} 's in a similar way. Using the approximate expression of probabilities in presence of NSI, writing down the expression for C_{12} in a compact form is a difficult task as there are large number of additional parameters. Moreover, it would not lead to any further insight on the nature of correlations or violation of the stationarity condition. The relative dependence on the NSI parameters can be gleaned from the expressions for oscillation probabilities given in Sec. 2.1.

3 Results

In this section, we use the latest best-fit values of the oscillation parameters given in Table 1. The neutrino mass ordering can be normal (NO) or inverted (IO). We assume NO for all the plots, unless stated otherwise. The LGI quantities K_3 and K_4 are then obtained using the joint probabilities. We take the initial neutrino flavour to be $|\nu_e\rangle$. Note that the energy is held fixed at $E = 1$ GeV in all the plots, unless stated otherwise.

To begin with, we first plot K_3 and K_4 as a function of ΔL for the case of two flavour neutrinos in Fig. 1. If we examine Eq. 16 carefully, we expect to get an oscillatory function of ΔL (for fixed E). The exact numerical results agree perfectly well with this observation. Clearly, there is an interplay of various C_{ij} 's which leads to an overall shape of K_3 and K_4 curves as a function of ΔL (see Fig. 1). From Fig. 1, we note that C_{12} (taken to be equal

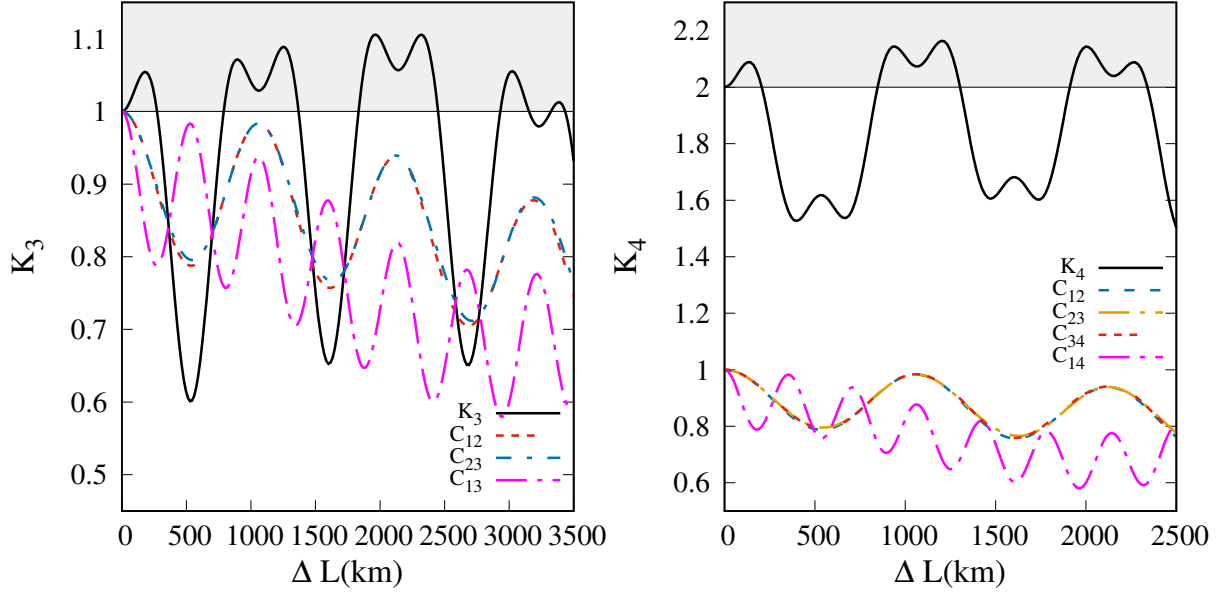


Figure 2: K_3 and K_4 plotted as a function of ΔL for the three flavour neutrino oscillations in matter with SI. The contribution of various C_{ij} 's is depicted in the two panels.

to C_{23}) dictates the overall frequency of K_3 and C_{13} leads to fine features. Likewise, C_{12} (taken to be equal to C_{23} and C_{34}) dictates the overall frequency of the K_4 and C_{14} leads to fine features. The joint probability terms appearing in C_{13} and C_{14} are responsible for the fine features of the overall curve (in black) for K_3 and K_4 respectively. We take $L_4 - L_3 = L_3 - L_2 = L_2 - L_1 \equiv \Delta L$ (see Ref. [32]). The largest violation of LGI is observed at the following values of ΔL :

$$K_3^{m,2fl} \simeq 1.433 \text{ at } \Delta L \simeq 160 \text{ km}, \dots 2090 \text{ km}$$

$$K_4^{m,2fl} \simeq 2.718 \text{ at } \Delta L \simeq 120 \text{ km}, \dots 2050 \text{ km}$$

It should be noted that in the two flavour case, the values of $K_3^{m,2fl}$ and $K_4^{m,2fl}$ are just below the respective maximal attainable bounds as given in Eq. 14.

In order to assess the role of NSI on the LGI for three flavour neutrino oscillations, we compute the oscillation probabilities numerically using the General Long Baseline Experiment Simulator (GLOBES) and associated implementation of NSI [54, 55]. The matter density has been taken to be 3 g/cc.

For the three flavour oscillations in matter with SI, the quantities K_3 and K_4 are plotted as function of ΔL in Fig. 2. Going from two- to three- flavour oscillations as shown in Fig. 2, we first note that the nice oscillatory feature is lost. This can be understood from the fact that stationarity condition is no longer maintained in this case. Also, in contrast to the two flavour case, the range of allowed values of K_3 and K_4 are modified. As mentioned earlier, the shape of the curves for K_3 and K_4 in case of SI are dictated by the interplay of the

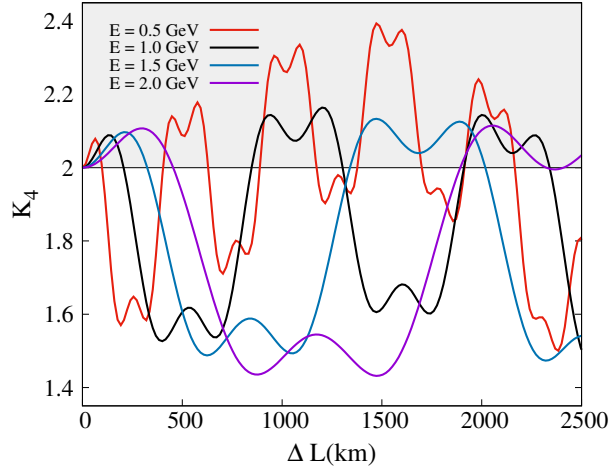


Figure 3: K_4 plotted as a function of ΔL for the three flavour neutrino oscillations in matter (SI case) for different values of E taken to be 0.5, 1.0, 1.5 and 2 GeV.

C_{ij} 's. Here again $L_4 - L_3 = L_3 - L_2 = L_2 - L_1 \equiv \Delta L$ and L_1 is chosen to be 140.15 km which maximises the LGI parameters, K_3 and K_4 [35]. The maximum violation of LGI in the standard case is found at the following values of ΔL :

$$K_3^m \simeq 1.106 \text{ at } \Delta L \simeq 1970 \text{ km \& } 2320 \text{ km}$$

$$K_4^m \simeq 2.163 \text{ at } \Delta L \simeq 1200 \text{ km}$$

Thus, as we go from two to three flavour case, the maximum values of LGI parameters, K_3^m and K_4^m are much smaller than the corresponding values ($K_3^{m,2fl}$ and $K_4^{m,2fl}$) obtained in the two flavour case.

In Fig. 3, we show the dependence of K_4 on the energy ($E = 0.5, 1.0, 1.5, 2.0$ GeV). Note that the E -dependence arises via factors such as $\lambda \propto 1/E$ and $r_A \propto E$ appearing in Eq. 18. It can be noted that the value of K_4 increases as we go to lower energies. Moreover, there is a shift in the value of ΔL at which the maximum violation occurs as the phase factors get modified with change in E . The maximum violation occurs for $E = 0.5$ GeV at $\Delta L \simeq 1500$ km.

$$K_4^m \simeq 2.393 \text{ at } \Delta L \simeq 1470 \text{ km for } E = 0.5 \text{ GeV}$$

$$K_4^m \simeq 2.163 \text{ at } \Delta L \simeq 1200 \text{ km for } E = 1.0 \text{ GeV}$$

$$K_4^m \simeq 2.133 \text{ at } \Delta L \simeq 1470 \text{ km for } E = 1.5 \text{ GeV}$$

$$K_4^m \simeq 2.115 \text{ at } \Delta L \simeq 2050 \text{ km for } E = 2.0 \text{ GeV}$$

Having found the location of maximum violation of LGI for two- and three- flavour neutrino oscillations, we first examine if the values of K_4 has any dependence on the the current unknowns in neutrino oscillation physics in Fig. 3. These unknowns are: (i) ordering

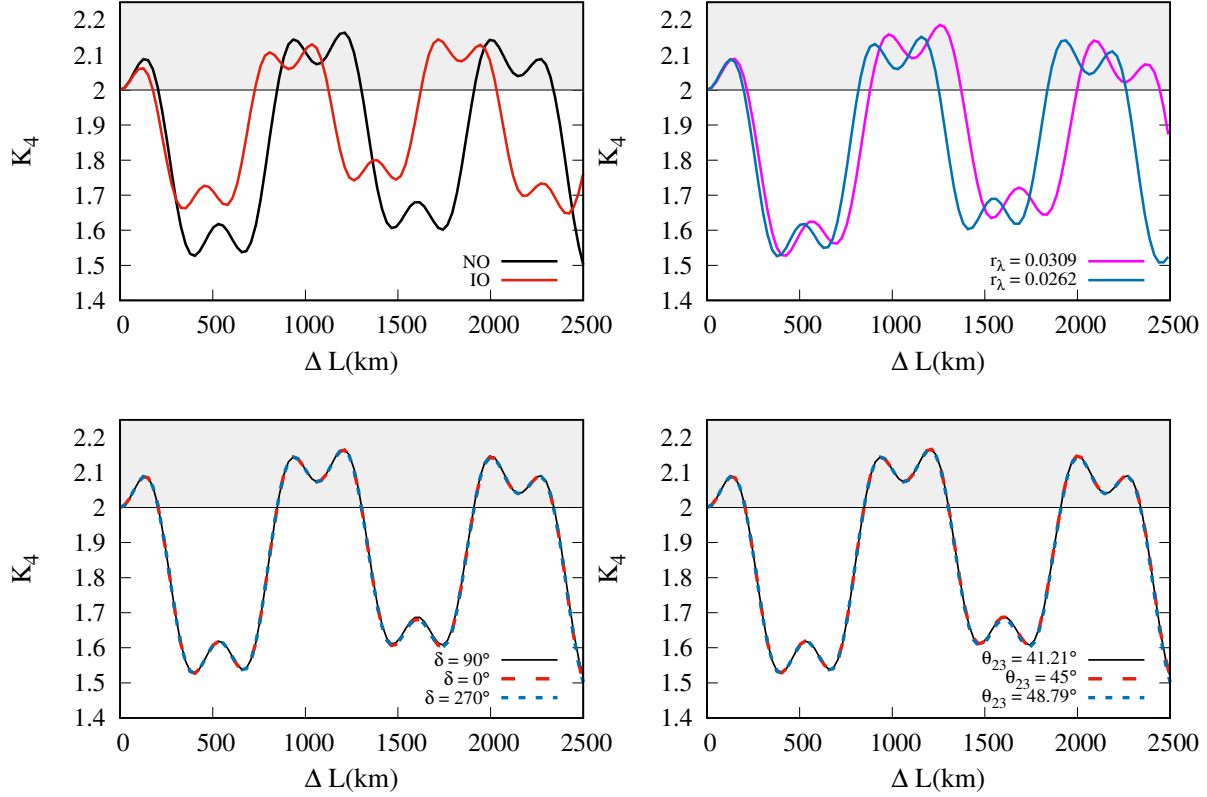


Figure 4: The dependence of K_4 on the current unknowns in neutrino oscillation physics - the ordering of neutrino masses (sign of Δm_{31}^2), the dependence on value of mass ordering parameter, r_λ in the allowed range (for NO), the value of the CP violating phase, δ and the octant of θ_{23} as a function of ΔL for three flavour neutrino oscillations in presence of SI.

of neutrino masses (sign of Δm_{31}^2) as shown in top row (left panel), (ii) the value of the CP violating phase, δ as shown in bottom row (left panel), and (iii) the octant of θ_{23} as shown in bottom row (right panel). It is seen that the height of the curve and shift in the location of maximum violation depends on the ordering of neutrino masses (sign of Δm_{31}^2). In general, for IO, the maximum value that K_4 attains is lower and given by $K_4^m \simeq 2.144$ at $\Delta L \simeq 1710$ km. There is mild dependence on value of δ and θ_{23} . Besides, in the top row (right panel), we also show the dependence on the value of mass ordering parameter, r_λ by varying its value within the allowed range for a given ordering (NO). It is noted that there is some dependence on the value of this parameter as it leads to change in the location (value of ΔL) of maximum violation as well as change in value of K_4^m . In order to understand the precise role of antineutrinos for a given ordering (NO) of neutrino masses, we expect that the curve for antineutrinos with NO would be similar to neutrinos with IO. This can be understood as follows. The effective combination entering the oscillation probability at the leading order [20] is r_A which is the ratio of A and Δm_{31}^2 and it does not matter whether we change $A \rightarrow -A$ (neutrinos \rightarrow antineutrinos) or the ordering of neutrino masses $\Delta m_{31}^2 \rightarrow -\Delta m_{31}^2$ (NO \rightarrow IO).

Next we analyse the impact of NSI on the LGI parameter, K_4 . We start by considering one NSI parameter non-zero at a time. This simplifies the computation and allows for a

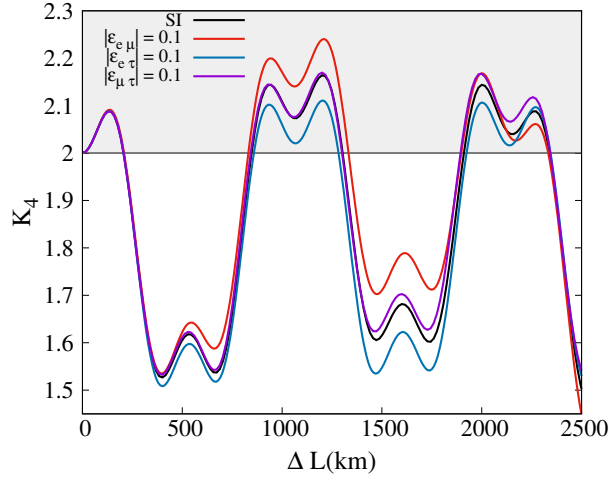


Figure 5: K_4 is plotted as a function of ΔL for three flavour oscillations in presence of NSI. Here, we take one NSI parameter non-zero at a time. The NSI phases are set to zero.

clear understanding of the role played by the specific NSI parameters. In Fig. 5, we show the impact of $|\varepsilon_{e\mu}|$, $|\varepsilon_{e\tau}|$ and $|\varepsilon_{\mu\tau}|$. We choose the strength of NSI terms to be $|\varepsilon_{\alpha\beta}| = 0.1$ for all the three NSI parameters so that we can compare their impact on similar footing. As can be noted from Fig. 5, the NSI terms, $|\varepsilon_{e\mu}|$ and $|\varepsilon_{e\tau}|$ act in the opposite directions which is expected from the analytic expressions of oscillation probabilities in the $\nu_\mu \rightarrow \nu_e$ channel given in Sec. 2.1 [56] and the difference is prominently seen in the grey shaded region that depicts violation of LGI. While $|\varepsilon_{e\mu}|$ leads to enhancement in the amount of violation of LGI with respect to the SI case, $|\varepsilon_{e\tau}|$ leads to suppression. As noted from Sec. 2.1, the parameter $|\varepsilon_{\mu\tau}|$ enters the expression for $\nu_\mu \rightarrow \nu_\mu$ channel. We find that the dependence of K_4 on $|\varepsilon_{\mu\tau}|$ is mild and closer to the expectation for the SI case. The NSI phases have been set to zero. This observed enhancement is the key point of this article. The maximum violation of LGI in the NSI case are observed at the following values of ΔL :

$$K_4^m \simeq 2.240 \text{ (2.331) for } |\varepsilon_{e\mu}| = 0.1 \text{ (0.2) at } \Delta L \simeq 1210 \text{ km}$$

It should be noted that K_4^m increases with the increase in the absolute value of the NSI term but still the value is below the maximal attainable bound (see Eq. 14). The impact of non-zero NSI phases ($\delta_{e\mu}$ and $\delta_{e\tau}$) while taking one NSI parameter non-zero at a time has been shown in Fig. 6. It can be seen that maximum violation in case of non-zero $\varepsilon_{e\mu}$ occurs for $\delta_{e\mu} = 0$. Also, the maximum violation in case of non-zero $\varepsilon_{e\tau}$ occurs for $\delta_{e\tau} = \pi$.

Motivated by the recent work on explaining the discrepancy between T2K and NoVA using large NSI [29, 30], we have plotted K_4 for the considered values of NSI terms. The impact of collective NSI terms ($\varepsilon_{e\mu}$ and $\varepsilon_{e\tau}$ along with non-zero phases, $\delta_{e\mu}$ and $\delta_{e\tau}$) is shown in Fig. 7. With the goal of maximizing the K_4 , the phases have been appropriately chosen using the insight obtained above (Fig. 6). The maximum violation of LGI in the NSI case (with $|\varepsilon_{e\mu}| = 0.2$, $|\varepsilon_{e\tau}| = 0.2$, $\delta_{e\mu} = 0$ and $\delta_{e\tau} = \pi$) is observed at the following value of ΔL :

$$K_4^m \simeq 2.481 \text{ at } \Delta L \simeq 1200 \text{ km for } \nu \text{ (} |\varepsilon_{e\mu}| = |\varepsilon_{e\tau}| = 0.2, \delta_{e\mu} = 0, \delta_{e\tau} = \pi \text{)}$$

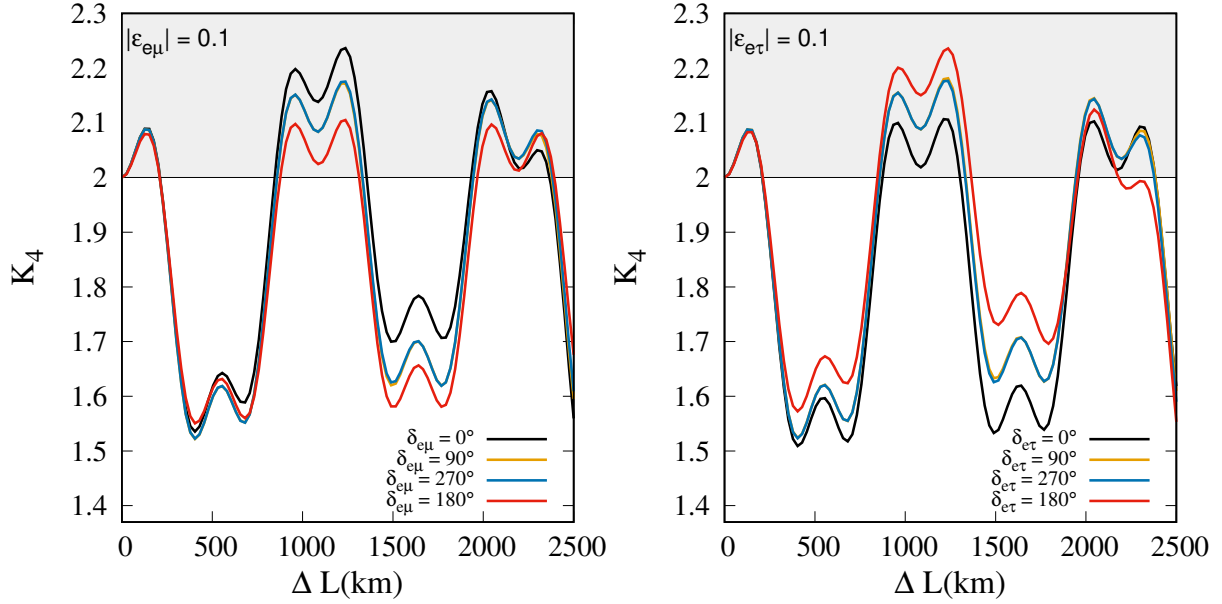


Figure 6: K_4 is plotted as a function of ΔL for three flavour oscillations in presence of NSI. Here, we take one NSI parameter non-zero at a time. The impact of corresponding NSI phases is depicted.

$$K_4^m \simeq 2.388 \text{ at } \Delta L \simeq 1000 \text{ km for } \bar{\nu} (|\varepsilon_{e\mu}| = |\varepsilon_{e\tau}| = 0.2, \delta_{e\mu} = \pi, \delta_{e\tau} = 0)$$

By making appropriate choice of NSI parameters, the value of K_4^m can reach upto a maximum of ~ 2.481 for $\Delta L \sim 1200$ km. In order to understand the case of antineutrinos for the same ordering, we know that the sign of the matter potential gets reversed as we go from neutrinos to antineutrinos, *i.e.*, $A \rightarrow -A$. Thus, the choice of NSI phases has to be carefully done, to see effects of enhancement in LGI violation. Finally, our key results are summarized in Table 2. It should be noted that we see an enhancement in the value of K_4^m from 2.163 (in case of SI) to 2.481 (for the considered NSI parameters) at around the same value of $\Delta L \sim 1200$ km. This amounts to $\sim 15\%$ relative change. However, as expected, the enhanced value still stays below the maximal attainable bound of $2\sqrt{2}$ (see Eq. 14).

4 Conclusion and outlook

That neutrino oscillations is quantum mechanical phenomenon is well-known. Unlike photons, they have extremely large mean free path and exhibit sustained coherence over astrophysical length scales. This provides for a unique opportunity to employ neutrinos as a useful quantum resource. However, in order to do so, one would require a thorough understanding of the aspects such as how neutrinos affect implications of LGI and its violation under different situations - propagation in vacuum as well as in matter with and without standard interactions. In this respect, there are several theoretical studies discussing two [32–34] and

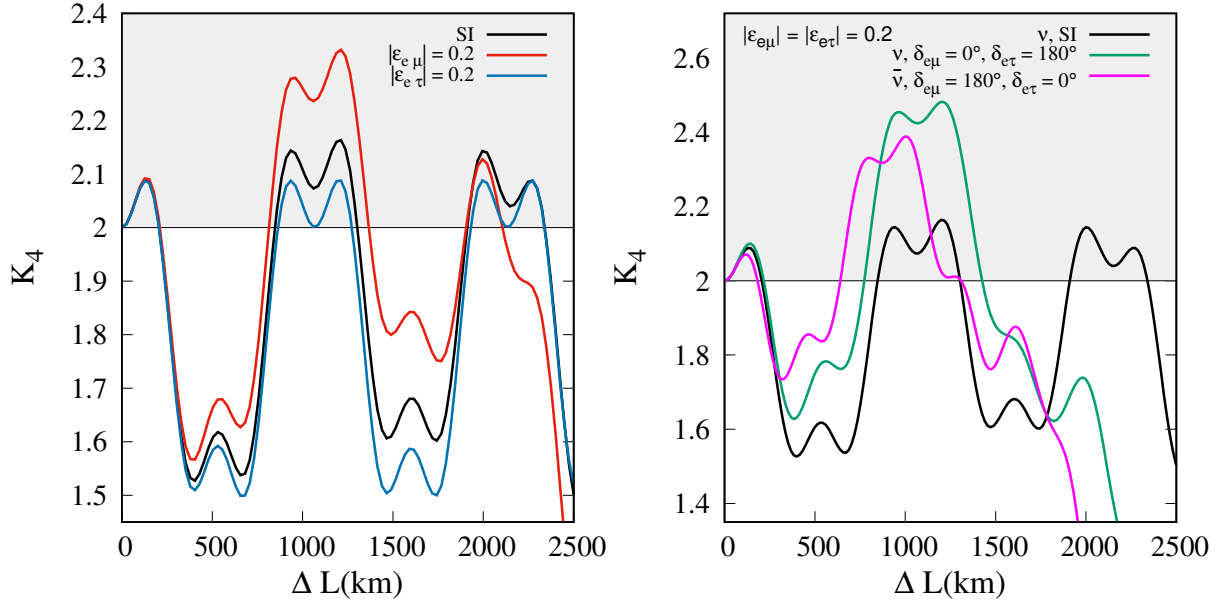


Figure 7: K_4 is plotted as a function of ΔL for three flavour oscillations in presence of NSI. Here, we take large values of NSI parameters. The role of individual NSI terms (taken to be real) in order to maximize K_4 is shown in the left panel. The role of collective NSI terms along with appropriate phase values in order to maximize K_4 is shown in the right panel.

Scenario	K_4^m	ΔL (km)	Relative change (%)
ν , SI	2.163	1200	0
ν , NSI ($ \varepsilon_{e\mu} = 0.1$)	2.240	1210	3.56
ν , NSI ($ \varepsilon_{e\mu} = 0.2$)	2.331	1210	7.77
ν , NSI ($ \varepsilon_{e\mu} = \varepsilon_{e\tau} = 0.2, \delta_{e\mu} = 0, \delta_{e\tau} = \pi$)	2.481	1200	14.7
$\bar{\nu}$, NSI ($ \varepsilon_{e\mu} = \varepsilon_{e\tau} = 0.2, \delta_{e\mu} = \pi, \delta_{e\tau} = 0$)	2.388	1000	10.40

Table 2: Maximum value of K_4 and corresponding value of ΔL for different scenarios. The relative change with respect to SI case (for neutrinos) is also mentioned in the table. NO is assumed.

three [35–38] flavour neutrino oscillations with and without the assumption of stationarity. Additionally, data from two experiments, MINOS and Daya Bay [33, 34] have been analysed using a two flavour approach in the context of LGI and a convincing result has been derived from these studies.

Currently, one of the primary goals of the ongoing and future experiments in neutrino oscillation physics are to get a handle on the unknowns - the CP phase (δ), neutrino mass

ordering (sign of Δm_{31}^2) and the octant of θ_{23} . Moreover, the precision of these experiments would allow for testing the existence of new physics in the form of NSI and/or allow for setting tighter constraints on the NSI parameters (see [26–28] for reviews). We go beyond these studies and explore the role of NSI on the violation of LGI. We show that the NSI effects could lead to an enhancement in the violation of LGI for appropriate choice of values of these parameters. It would be worthwhile to explore the impact of NSI in neutrino oscillations via other measures of quantumness such as quantum witness or contextuality [10–14].

It should be noted that in order to measure the LGI parameter, conventionally, one needs a minimum of three time measurements (for K_3). For higher order LGI parameters (K_n), we will need four and more such measurements. This means that one requires at least three baselines with identical detection possibilities to infer the simplest of LGI parameters, K_3 . However, it is practically impossible to realize the three baseline measurement experimentally. The value of $\Delta L \simeq 1200$ km where large enhancement in K_4 is found does not imply a fixed baseline experiment and should not be confused with any particular experiment.

A way to tackle this problem has been put forth by Formaggio et al for two flavour case [33]. The authors used the fact that in the phase factor one has two experimental handles - one is the L and other one is the E which can be independently tuned. One can mimic the change in L by a corresponding change in E . This is how the authors performed a test of LGI using data from MINOS experiment with $L = 735$ km, by selecting various energies E_a for measurements such that the phases obeyed a certain sum rule. Thus, using similar approach, if we can observe enhanced violation in data from a fixed baseline experiment such as DUNE, then that will be indicative of the presence of new physics.

In the present work, we take $|\nu_e\rangle$ as the initial state and discuss the role of current unknowns in neutrino oscillation physics as well as role of antineutrinos in our inferences about LGI violation. We then go on to investigate the impact of NSI on the violation of LGI. In the existing studies related to testing LGI in neutrino oscillations, different initial states have been employed. For instance, $|\nu_\mu\rangle$ was used as an initial state in studies pertaining to LGI for two and three flavour neutrino oscillations [36–38] as well as in establishing 6σ evidence for violation of LGI in two flavour context using data from MINOS experiment [33]. $|\nu_e\rangle$ was used as an initial state in [32, 35]. While it is found that LGI is violated in all these studies irrespective of the source type, it would be worthwhile to carry out a detailed study with different possible source types and investigate their impact on the violation of LGI.

There are discussions on the possibility to manipulate neutrinos for the purpose of communications, such as galactic neutrino communication [57] and submarine neutrino communication [58]. Stancil et al. reported on the performance of a low-rate communications link established using the NuMI beam line and the MINERvA detector illustrating the feasibility of using neutrino beams to provide low-rate communications link [59]. Synchronized neutrino communications over intergalactic distances have been studied in [60]. Of course, the scales of these studies is completely different and averaging of neutrino oscillations will have different manifestations on questions such as LGI and quantum coherence. Temporal correlations of the LGI kind might give additional handle to extend these studies.

Acknowledgements

We acknowledge useful discussions with Ipsika Mohanty and Animesh Sinha Roy during various stages of this work. The use of HPC cluster at SPS, JNU funded by DST-FIST is acknowledged. SS acknowledges financial support in the form of fellowship from University Grants Commission. PM would like to acknowledge funding from University Grants Commission under UPE II at JNU and Department of Science and Technology under DST-PURSE at JNU. The work of PM is partially supported by the European Union's Horizon 2020 research and innovation programme under the Marie Skłodowska-Curie grant agreement No 690575 and 674896.

References

- [1] P. A. M. Dirac, *The Principles of Qunatum Mechanics (third edition)* (The Clarendon Press, Oxford, 1947).
- [2] Y. Aharonov and D. Bohm, Phys. Rev. **115**, 485 (1959).
- [3] J. S. Bell, Rev. Mod. Phys. **38**, 447 (1966).
- [4] A. J. Leggett and A. Garg, Phys. Rev. Lett. **54**, 857 (1985).
- [5] C. Emary, N. Lambert, and F. Nori, Rep. Prog. Phys. **77**, 016001 (2013).
- [6] B. S. Cirelson, Lett. Math. Phys. **4**, 93 (1980).
- [7] C. Budroni, T. Moroder, M. Kleinmann, and O. Gühne, Phys. Rev. Lett. **111**, 020403 (2013).
- [8] C. Budroni and C. Emary, Phys. Rev. Lett. **113**, 050401 (2014).
- [9] D. Rohrlich and S. Popescu, in *60 Years of EPR: Workshop on the Foundations of Quantum Mechanics (In Honor of Nathan Rosen)* (1995), quant-ph/9508009.
- [10] T. Baumgratz, M. Cramer, and M. B. Plenio, Phys. Rev. Lett. **113**, 140401 (2014).
- [11] A. Winter and D. Yang, Phys. Rev. Lett. **116**, 120404 (2016).
- [12] M. Ban, International Journal of Theoretical Physics **58**(9), 2893 (2019).
- [13] A. Friedenberger and E. Lutz, Phys. Rev. A **95**, 022101 (2017).
- [14] J. J. Mendoza-Arenas, F. J. Gómez-Ruiz, F. J. Rodríguez, and L. Quiroga, Scientific Reports **9**(1), 17772 (2019).
- [15] Z. Maki, M. Nakagawa, and S. Sakata, Prog. Theo. Phys. **28**(5), 870 (1962).
- [16] B. Pontecorvo, Sov. Phys. JETP **7**, 172 (1958).
- [17] B. Pontecorvo, Sov. Phys. JETP **6**, 429 (1957).

- [18] V. Gribov and B. Pontecorvo, Phys. Lett. B **28**, 493 (1969).
- [19] T. Kajita and A. B. McDonald, *For the discovery of neutrino oscillations, which shows that neutrinos have mass*, the Nobel Prize in Physics 2015. <https://www.nobelprize.org/prizes/physics/2015/summary/>.
- [20] C. Giunti and C. W. Kim, *Fundamental of Neutrino Physics and Astrophysics* (World Scientific, Singapore, 2004).
- [21] L. Wolfenstein, Phys. Rev. D **17**, 2369 (1978).
- [22] L. Wolfenstein, Phys. Rev. D **20**, 2634 (1979).
- [23] J. W. F. Valle, Phys. Lett. B **199**, 432 (1987).
- [24] M. M. Guzzo and S. T. Petcov, Phys. Lett. B **271**, 172 (1991).
- [25] E. Roulet, Phys. Rev. D **44**, 935 (1991).
- [26] T. Ohlsson, Rept. Prog. Phys. **76**, 044201 (2013).
- [27] Y. Farzan and M. Tortola, Front.in Phys. **6**, 10 (2018).
- [28] *Neutrino Non-Standard Interactions: A Status Report*, vol. 2, 1907.00991.
- [29] S. S. Chatterjee and A. Palazzo, Phys. Rev. Lett. **126**(5), 051802 (2021).
- [30] P. B. Denton, J. Gehrlein, and R. Pestes, Phys. Rev. Lett. **126**(5), 051801 (2021).
- [31] P. Mehta, Phys. Rev. D **79**, 096013 (2009).
- [32] D. Gangopadhyay, D. Home, and A. S. Roy, Phys. Rev. **A88**(2), 022115 (2013).
- [33] J. A. Formaggio, D. I. Kaiser, M. M. Murskyj, and T. E. Weiss, Phys. Rev. Lett. **117**(5), 050402 (2016).
- [34] Q. Fu and X. Chen, Eur. Phys. J. **C77**(11), 775 (2017).
- [35] D. Gangopadhyay and A. S. Roy, Eur. Phys. J. **C77**(4), 260 (2017).
- [36] J. Naikoo, A. K. Alok, S. Banerjee, S. Uma Sankar, G. Guarnieri, C. Schultze, and B. C. Hiesmayr, Nucl. Phys. B **951**, 114872 (2020).
- [37] J. Naikoo, A. K. Alok, S. Banerjee, and S. U. Sankar, Phys. Rev. D **99**, 095001 (2019).
- [38] J. Naikoo, S. Kumari, S. Banerjee, and A. Pan, J. Phys. G **47**(9), 095004 (2020).
- [39] X.-K. Song, Y. Huang, J. Ling, and M.-H. Yung, Phys. Rev. A **98**(5), 050302 (2018).
- [40] F. Ming, X.-K. Song, J. Ling, L. Ye, and D. Wang, Eur. Phys. J. C **80**(3), 275 (2020).
- [41] M. Richter, B. Dziewit, and J. Dajka, Phys. Rev. D **96**(7), 076008 (2017).
- [42] M. Richter-Laskowska, M. Lobejko, and J. Dajka, New J. Phys. **20**(6), 063040 (2018).

- [43] K. Dixit, J. Naikoo, S. Banerjee, and A. Kumar Alok, Eur. Phys. J. C **79**(2), 96 (2019).
- [44] K. Dixit and A. K. Alok, The European Physical Journal Plus **136**(3), 334 (2021).
- [45] D. Wang, F. Ming, X.-K. Song, L. Ye, and J.-L. Chen, Eur. Phys. J. C **80**(8), 800 (2020).
- [46] A. K. Jha, S. Mukherjee, and B. A. Bambah, Mod. Phys. Lett. A **36**(09), 2150056 (2021), 2004.14853.
- [47] P. F. de Salas, D. V. Forero, S. Gariazzo, P. Martínez-Miravé, O. Mena, C. A. Ternes, M. Tórtola, and J. W. F. Valle, JHEP **02**, 071 (2021).
- [48] S. Davidson, C. Pena-Garay, N. Rius, and A. Santamaria, JHEP **03**, 011 (2003), hep-ph/0302093.
- [49] C. Biggio, M. Blennow, and E. Fernandez-Martinez, JHEP **08**, 090 (2009), 0907.0097.
- [50] J. Kopp, M. Lindner, T. Ota, and J. Sato, Phys. Rev. D **77**, 013007 (2008), 0708.0152.
- [51] T. Kikuchi, H. Minakata, and S. Uchinami, JHEP **03**, 114 (2009), 0809.3312.
- [52] K. Asano and H. Minakata, JHEP **06**, 022 (2011), 1103.4387.
- [53] P. Zucchelli, Physics Letters B **532**(3), 166 (2002).
- [54] P. Huber, M. Lindner, and W. Winter, Comput. Phys. Commun. **167**, 195 (2005).
- [55] P. Huber, J. Kopp, M. Lindner, M. Rolinec, and W. Winter, Comput. Phys. Commun. **177**, 432 (2007).
- [56] M. Masud, A. Chatterjee, and P. Mehta, J. Phys. **G43**(9), 095005 (2016).
- [57] J. G. Learned, S. Pakvasa, and A. Zee, Phys. Lett. B **671**, 15 (2009).
- [58] P. Huber, Phys. Lett. B **692**, 268 (2010).
- [59] D. Stancil *et al.* (MINERvA), Mod. Phys. Lett. A **27**, 1250077 (2012).
- [60] A. Santos, E. Fischbach, and J. Gruenwald (2020), 2007.05736.